J. Earth Syst. Sci. (2020)129 5
https://doi.org/10.1007/s12040-019-1286-3

Thermal anomalies detection before Saravan earthquake (April 16th, 2013, $M_W = 7.8$) using time series method, satellite, and meteorological data

Marzieh Khalili[1,*], Seyed Sabereh Abdollahi Eskandar[1] and Seyed Kazem Alavi Panah[2]

[1]*Department of Earth Sciences, College of Sciences, Shiraz University, Shiraz, Iran.*
[2]*Department of Remote Sensing and GIS, Faculty of Geography, Tehran University, Tehran, Iran.*
**Corresponding author. e-mail: marzieh-khalili@shirazu.ac.ir*

MS received 9 September 2018; revised 16 June 2019; accepted 25 August 2019

Thermal anomaly detection related to strong earthquakes is one of the earthquake precursors extensively investigated by researchers. In this research, five years (March 16th to May 16th, every year from 2009 to 2013) of Land Surface Temperature (LST) data products, obtained from satellite data (MODIS-Aqua), and meteorological data (air and soil temperature), using three-dimensional time series method, have been analyzed to characterize the thermal anomalies related to the Saravan earthquake (April 16th, 2013, $M_w = 7.8$). The results indicate that the thermal anomalies were observed in the time period before and after the earthquake. In the LST time–space–temperature coordinates, the thermal anomaly pattern was seen before the Saravan earthquake. In the Kriging surfaces of the air temperature and the difference between the LST and air temperature (ΔT), considerable changes were seen a few days before the earthquake until a few days after it. In addition, the soil temperature time–space–temperature coordinates show changes (increase) a few days after the Saravan earthquake. Therefore, the obtained results suggest that these changes (thermal anomalies) are related to the earthquake and can be expressed as an earthquake predictor.

Keywords. Earthquake precursor; thermal anomaly; time series; land surface temperature; meteorological data; Iran.

1. Introduction

Earthquake is one of the most devastating natural disasters that sometimes occurs without any warning, although some earthquakes are accompanied by some changes. Such changes occurring before or during an earthquake on lithosphere, atmosphere and ionosphere are known as earthquake precursory (Molchanov and Hayakawa 2008).

A wide range of predictors including variations in seismicity patterns, ground deformations (uplift and tilt), ion clouds, thermal changes, electromagnetic anomalies, and Total Electron Content (TEC) have been witnessed before major earthquakes (e.g., Pulinets 1997; Cicerone *et al.* 2009; Crockett and Gillmore 2010; Guangmeng and Jie 2013; Li and Parrot 2013; Eleftheriou *et al.* 2016).

Theoretically, all the mechanical energy stored in the crust is not released during an earthquake, but some of it is transformed into other forms of energy (e.g., electrical energy and thermal energy) (Freund 2003).

Published online: 19 December 2019

There are different theories accounting for thermal anomalies before an earthquake, including the emission of gas from the ground (Qiang *et al.* 1997, 1999; Freund 2009), changes in underground water levels (Asteriadis and Livieratos 1989; ZiQi *et al.* 2002), and the ionization of the air by radon (Pulinets *et al.* 2006). However, factors other than an earthquake can cause anomalies in satellite images. These factors include surface spectral emissivity, atmospheric spectral transmittance, surface temperature (spatial and temporal changes), and observational conditions (temporal variations of satellite zenithal angle), etc. (Tramutoli *et al.* 2015).

In addition, thermal patterns may be related to certain processes including the earth's motion relative to the sun, climatic, atmospheric and physical factors, topography, geological layers, and the presence of water and plants (Pavlidou 2013). These thermal patterns are expressed as normal thermal profiles.

Determining the characteristics of thermal anomalies before an earthquake is of great importance, and it should be distinguishable from the expected normal form (Chandola *et al.* 2009). The first study on thermal anomalies, using satellite images before an earthquake, was conducted by Gorny *et al.* (1988). After that, many studies with improved earthquake's data (with wide range of magnitudes (from 4.0 to 7.9)) obtained from different satellite sensors (AVHRR/NOAA, etc.) and methods in various geological settings across the world have confirmed a strong relationship between thermal anomalies and the occurrence of earthquakes (e.g., Qiang *et al.* 1997; Tronin *et al.* 2002, 2004; Di Bello *et al.* 2004; Corrado *et al.* 2005; Aliano *et al.* 2008; Saraf *et al.* 2009; Tramutoli *et al.* 2015; Eleftheriou *et al.* 2016; Khalili *et al.* 2019; Saber Mahani and Khalili 2019). Thermal anomalies have been identified not only before the occurrence of an earthquake but also in the phase of seismic and aftershocks. These can be used as a predictor in short-term prediction studies.

In addition, some researchers were comprised the meteorological and satellite data in order to investigate the relationship between thermal anomalies and the occurrence of earthquakes, e.g., Prigent *et al.* (2003), Choudhury *et al.* (2006), and Mildrexler *et al.* (2011).

The main aim of this research is to investigate the existence of thermal anomalies related to the Saravan earthquake using a three-dimensional time series method and LST data obtained from MODIS satellite (March 16th to May 16th, every year from 2009–2013). Furthermore, using air and soil temperature data taken from meteorological stations in the same time period (March 16th to May 16th, every year from 2009 to 2013), thermal anomalies related to the earthquake were analyzed and compared with the satellite data.

2. Case study region

According to the Dobrovolsky *et al.* (1979) formula (equations 1 and 2), earthquakes with magnitudes greater than 4 on the Richter scale occur within a given distance from thermal anomalies. Estimation of deformation and tilting of the earth's surface is considered as a function of the earthquake's magnitude (M) and the distance from the earthquake's epicenter (D). It is assumed that the area affected by deformation is a circle whose center is the earthquake's epicenter. The radius of the circle (RD) is estimated as the strain radius.

$$RD = 10^{0.43M}\,\text{km}, \tag{1}$$

$$150 \leq D \leq RD. \tag{2}$$

Based on the formula, the study area with 26°30′–29°30′N latitude and 60°30′–63°30′E longitude was selected. The study area center is being the Saravan earthquake (figure 1). This region is located partly in the southeast of Iran, the Makran zone (Zamani *et al.* 2011), and partly in the Balochistan province of Pakistan (figure 1).

Tectonics and seismotectonics of the Makran zone are discussed by some researchers and identified as an active subduction zone, e.g., Quittmeyer and Jacob (1979), Schluter *et al.* (2002), Vernant *et al.* (2004), Haghipour *et al.* (2012), Barnhart *et al.* (2014), and Abedi and Bahroudi (2016).

The main seismotectonic features of the region are the Saravan Fault, Mashkel Fault, and Lagdasht Fault (figure 1). Based on seismic hazard zonation, this region has a low level of hazard for the future occurrence of a number of earthquakes with $M_b \geq 4.5$ Richter (Zamani *et al.* 2012; Khalili and Zamani 2016).

The study area is a mountainous area with no significant agricultural land (the presence of plants may change the temperature in a region). The weather condition of the region based on De Martonne climate type is dry (Tabari *et al.* 2014). According to Rashki (2012), and Iran Meteorological

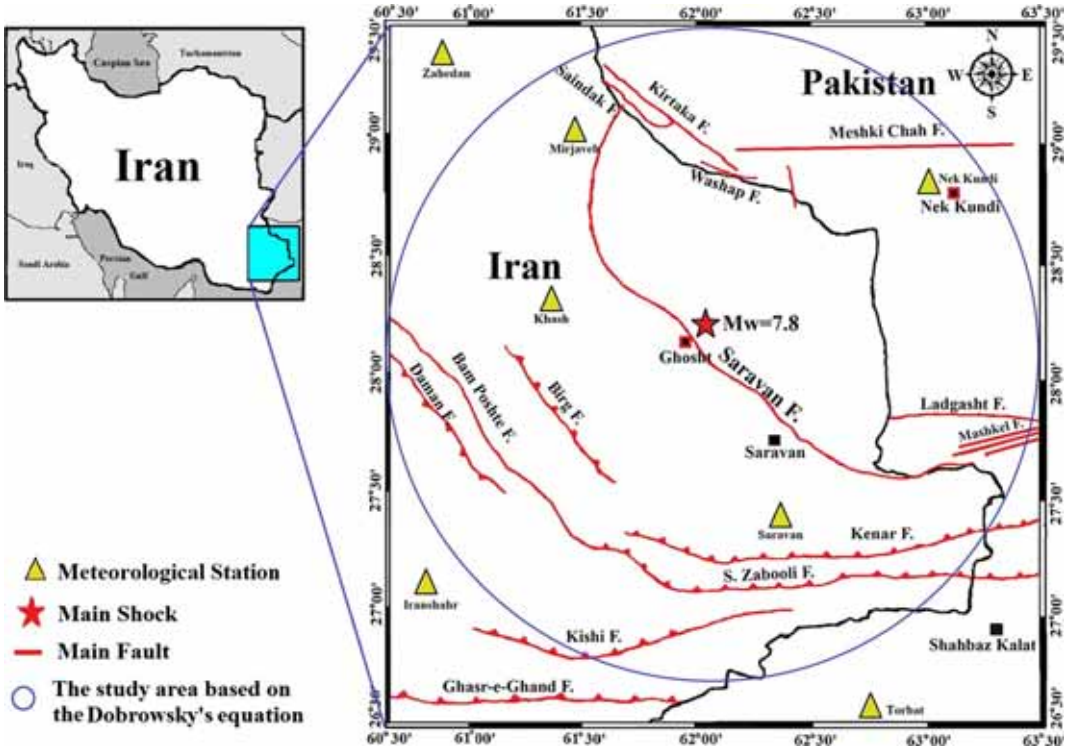

Figure 1. The study area map indicates the locations of the main faults and the meteorological stations.

Organization data, the studied area has suffered from drought (very low humidity) from 2000 to 2018. In addition, no major fires have been reported in the region during the time of the study (2009 up to 2013). Therefore, at the time of the study, there was no important source of thermal anomalies available.

3. Method and data

3.1 *Time series method*

In time series, the signal of anomalous events and their sequences can be identified and compared with normal time series. The identification of anomaly is done by tracing part of the data that have deviated from normal behavior. The boundary between normal and abnormal behavior is not always clear, and the normal pattern is not always stable and may evolve. In addition, abnormal behavior processes may be correlated with each other.

There are numerous methods to identify an anomaly in time series, including sequences, Markov, and hidden window based techniques. Before applying any method, a transformation, which improves the efficiency of anomaly identification in time series, may be performed. The transformations including aggregation (replacing the values of a set by their mean), discretization (sequencing continuous small values as discrete values), processing of signals (Fourier transform wavelet), and decreasing the dimensions of a series.

In this study, after the pre-processing and normalization of the data, the three research approaches are used to visualize and analyze the thermal patterns (figure 2). The first ones aim to diagnose land surface temperature anomalies in space–time. The second approach is used to diagnose thermal anomaly, using the difference between LST and air temperature 'ΔT'. This difference is explained by Sulce (2013) as follows (equation 3):

$$\Delta T = T_{\mathrm{L}} - T_A, \tag{3}$$

where T_{L} is the average LST in an area of 4 km^2 around the meteorological station and T_{A} is the air temperature recorded in the meteorological station.

The third approach is used to investigate soil temperature changes in time and space. Therefore, a system of time–space–temperature coordinates (3D diagram) was defined as an interpolated level (using an ordinary Kriging interpolation method) in order to investigate thermal anomaly pattern in

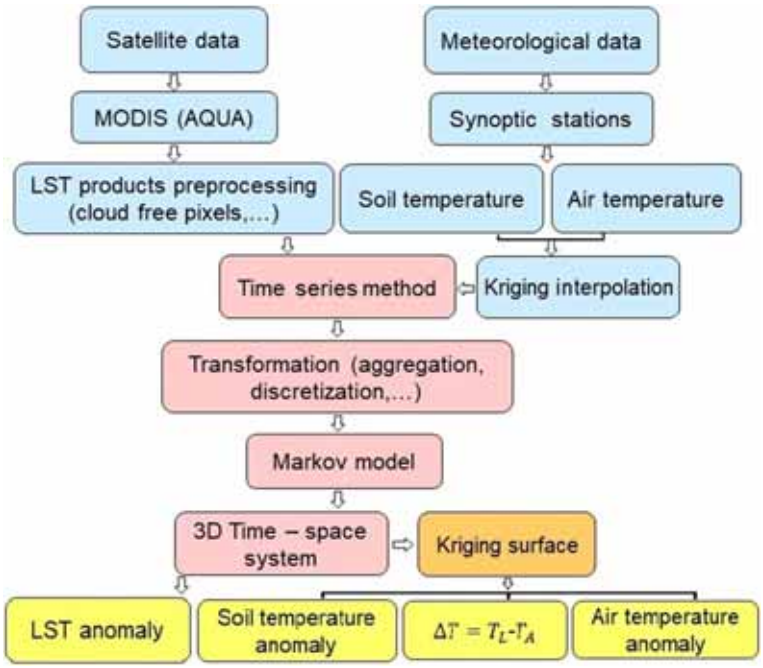

Figure 2. The flowchart of the methodology.

terms of time '*t*' (the day of the earthquake) and location '*d*' (distance from the epicenter of the earthquake). Temperature is automatically related to place and can be interpolated through the location.

When, data from a complete space coordinate system, such as the coordinate system of satellite imagery transfer to the time–space system, some information about the location may be lost. Therefore, to preserve the maximum geographical area in the satellite image, the study area was divided into two parts, the north, and the south areas. The stations located in the north of the earthquake's epicenter, are valued as positive on the diagram and the stations located in the south of the epicenter, are valued as negative (Sulce 2013). The diagrams show seasonal temperature patterns in different areas.

3.2 *Kriging interpolation method*

Kriging is an interpolation method which is derived from regionalized variable theory (Oliver and Webster 1990). In this method, the value of a function at a given point, predicts by computing a weighted average of the known values in the neighborhood of the point. One of the most commonly used Kriging methods is ordinary Kriging method. The major characteristic of ordinary Kriging is that it not only provides estimations with the minimum error but also predicts the error amounts.

3.3 *Land surface temperature (LST)*

Thermal remote sensing is a branch of remote sensing science that is concerned with processing and interpreting data and images obtained from one or more channels within Thermal Infra-Red (TIR) (8–14 μm) satellite imagery and electromagnetic (EM) spectrum. In thermal remote sensing, the radiation emitted from the surface of the phenomenon is measured (Alavipanah *et al.* 2017).

The LST satellite data are less influenced by atmospheric water vapor variability. Therefore, the use of LST data instead of TIR radiances at the sensor was proposed by Lisi *et al.* (2015).

The unusual increase in Land Surface Temperature (LST) has an important role in thermal anomalies detection a few days before and after major earthquakes. Numerous reports from various parts of the world have indicated an increase in land surface temperature (2–4°) during the time period 2–10 days before the earthquake and a few days after it in areas hit by an earthquake (near faults or tens to thousands of kilometers away from the earthquake's epicenter) (Pavlidou 2013).

In this study, satellite images (the LST products generated by NASA's Moderate Resolution Imaging Spectroradiometer (MODIS) Aqua (collection 5.1, (MYD11-L2A) with 1 km of spatial resolution)) for the time period from 2009 to 2013 (March 16th to May 16th) at the same night-time (20.30′–22.30′ GMT) were continuously used to determine changes in the LST. The remote sensing air temperature estimates are strongly influenced by errors on LST retrievals. Therefore, it is important to eliminate low-quality data. The reliability of the LST data is determined by the quality flags. Based on the quality flags, the pixels flagged with Average Emissivity Error < 0.04, and >0.02 or LST Error > 3 K, were eliminated (Benali *et al.* 2012).

Images with more than 80% Nan-data are excluded from the study (because these images did not capture part of the area or the pixels were cloudy). In order to reduce seasonal and sun light effects, night-time images for each month were used. In this research, only cloud-free pixels of each scene of the same data set were processed.

The images were generalized using the split-window algorithm to recover the LST data (Wan 2006). The function of this algorithm is to optimize LST data and eliminate its atmospheric effects, based on the differential absorption in adjacent infrared bands (Wan and Dozier 1996). The data are calibrated in terms of geographic location, cloud cover, atmospheric profile, land cover, and snow (Wan 2008). LST products are less affected by atmospheric water vapor variability (Lisi *et al.* 2015).

The LST data have been validated with *in-situ* measurements in the temperature range from –10°C to 58°C in more than 50 clear sky cases (Wan 2006) by the data providers.

3.4 *Meteorological data*

The solar energy, which hits the surface of the earth, warms the top shallow layer of the ground (3 cm). Any source of heat under the ground can increase the difference between the land surface temperature and air temperature. This difference, which is at a minimum during the night, can be investigated in a time–space series. In fact, at night-time, the LST is very close to the air temperature and sometimes below it (Mildrexler *et al.* 2011).

After deleting daily solar flux variations in relation to LST dataset and the air temperature, in good synoptic and even cloudy conditions, a difference in temperature of 2.9 K, can be observed before an earthquake (Prigent *et al.* 2003; Mildrexler *et al.* 2011).

In this research, the meteorological data including daily night-time air temperature, at a distance of 2 m above ground level, were taken from synoptic meteorological stations. The data were collected from all existence meteorological stations, spread through the study area (5 stations in Iran, and 2 stations in Pakistan) from the same period of time as in the case of LST satellite images (March 16th to May 16th, every year from 2009 to 2013).

In addition, ascending transfer of gases from the earth's surface through very fine pores (Saraf *et al.* 2009) and an increase in water level in wells due to an increase in ground temperature before an earthquake (Ouzounov *et al.* 2006) are among phenomena which are claimed to increase the temperature in the earth's surface and soil before an earthquake.

In order to study thermal anomaly in soil before the earthquake, the night-time soil temperature from points as deep as 5 cm obtained from the seven meteorological stations in the study area were continuously taken in a time period from 2009 to 2013 (March 16th to May 16th).

The diurnal modeling of air temperature (105 synoptic stations in Iran during the years 2013–2014), in relation to the environmental variables like humidity, pressure, diurnal temperature range, and wind speed was implemented and analyzed by Gholamnia *et al.* (2018). The results indicate that the spatio-temporal behaviors of wind and humidity, in the present study area, have a low variation in the time of the study (March 16th to May 16th).

4. Results and discussion

4.1 *Diagnosing thermal anomaly in the land surface temperature*

In this study, satellite images for the time period from 2009 to 2013 (March 16th to May 16th) were continuously used to determine changes in the LST.

After all of the images were pre-processed, the average of the LST was extracted from all of the images. Then a system of LST time–space–temperature coordinates has been created to investigate the LST thermal anomaly pattern in

terms of time '*t*' (the day of the earthquake), and location '*d*' (distance from the epicenter of the earthquake). Temperature is automatically related to place and can be interpolated through location (figure 3). It should be mentioned that in all of the graphs, days were represented on the horizontal axis as time, and distance from the epicenter in kilometer on the vertical axis.

As figure 3 shows, a warm pattern has emerged in the dotted area, which shows thermal anomaly before and after the earthquake. Although such patterns, can be seen in the specified areas in other years, the intensity and spread of the pattern in the year 2013, is bigger than the corresponding period in previous years, especially from April 12th to 16th. Moreover, in this year, the thermal pattern outside the area has returned to its previous pattern, but, for example, in the year 2010, which was generally a warmer year, this pattern has emerged outside the area and continued.

4.2 *Diagnosing thermal anomaly using the difference between the land surface temperature and air temperature*

In this research, the night-time LST and the air temperature, obtained from the seven meteorological stations that have sensors for measuring the temperature at 2 m above the surface of the ground, were used.

To illustrate thermal anomaly, it is necessary to draw an anomaly on the three-dimensional time–space coordinate system, where '*t*' shows time on the horizontal axis, '*d*' shows the station's distance from the epicenter of the earthquake on the vertical axis, and 'ΔT' (equation 3) shows the difference between the LST and the air temperature in color as the Kriging surfaces in figure 4.

As can be seen in figure 4, there is a great difference between the LST and the air temperature around the epicenter in the specified area, a day before until a few days after the Saravan earthquake.

By studying the LST and T_A data for all the time periods (March 16th to May 16th, from 2004 to 2013), it is revealed that both sets of data in the time period of the earthquake (2013) show a higher level in comparison with the other years, and this large difference in ΔT during the year 2013 is caused both by the high levels of LST and T_A. The fact is that the air temperature compared with the LST was high during the whole period, and it is possible that it is the air temperature that shows thermal anomaly, not the LST and researchers believe that air temperature can be introduced as thermal anomaly precursory (Sulce 2013).

In order to investigate the reason for the high level of ΔT and to test the hypothesis which indicate that the air temperature can be used as a predictor, the air temperature data from all the meteorological stations in the study area, (March 16th to May 16th, every year from 2009 to 2013) as interpolated surfaces, are shown in a time–space coordinate system (figure 5). A temperature surface was generated using ordinary Kriging interpolation method.

As figure 5 shows, a warm thermal pattern can be seen in the dotted area, which shows thermal anomaly before and after the earthquake. Although, a similar thermal pattern is repeating in all the periods, except in the year 2013, which the highest amounts of temperature can be seen from April 19th to 23rd, while it is at the lowest level for

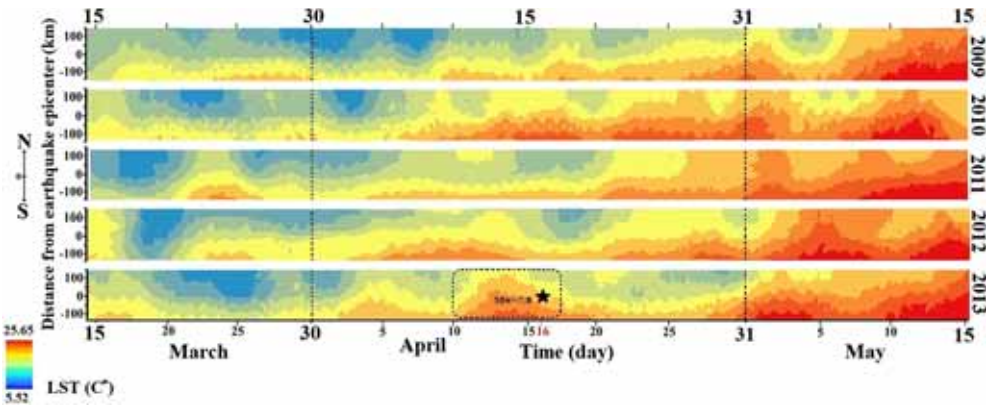

Figure 3. A system of LST time–space–temperature coordinates; temperature is automatically related to place and can be interpolated through the location. The region which is marked with black dots shows thermal anomalies.

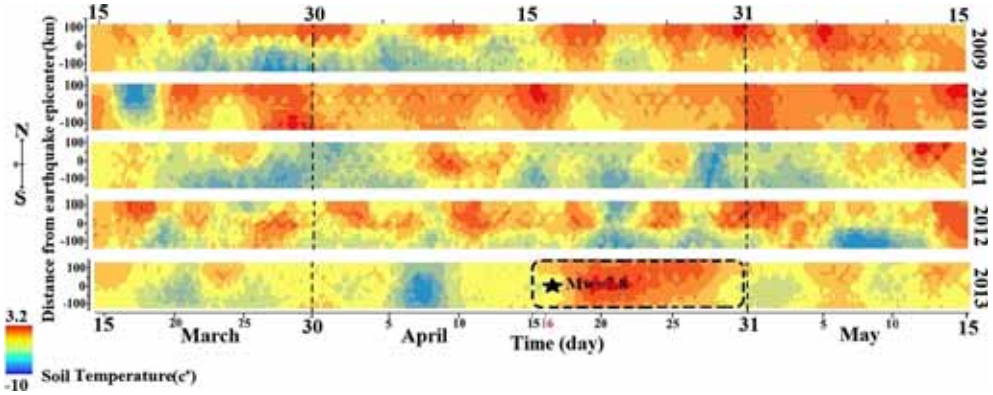

Figure 4. A system of the Kriging surfaces of the ΔT time–space–temperature coordinates; the temperature is automatically related to place and can be interpolated through the location. The region which is marked with black dots shows thermal anomalies.

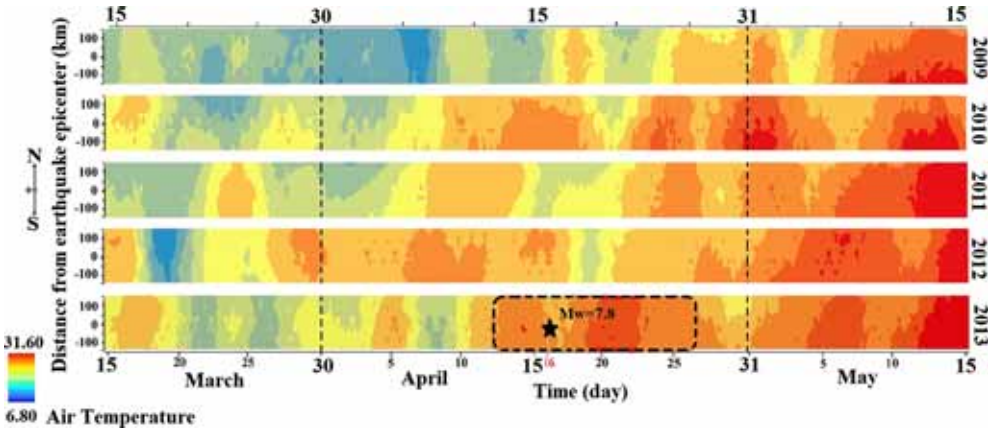

Figure 5. A system of the Kriging surfaces of the air temperature (T_A) time–space–temperature coordinates, temperature is automatically related to place and can be interpolated through the location. The region which is marked with black dots shows thermal anomalies.

the same time in the previous years. This indicates that this pattern is a seasonal pattern, which has also been repeated in the previous years and is caused by a climate cycle. However, a considerable change can be seen within the time period from 3 days before the earthquake until 10 days after it. It can be related to the Saravan earthquake.

4.3 *Investigating soil temperature changes in time and space*

In this research, to study thermal anomaly in soil before the earthquake, the night-time soil temperature from points as deep as 5 cm obtained from the seven meteorological stations in the study area were continuously taken in a time period from 2009 to 2013 (March 16th to May 16th) and are presented in the form of a time–space coordinate system (figure 6).

The triple data of the station's distance from the earthquake's epicenter, day, and soil temperature 'T_S' for the seven meteorological stations were extracted every day in a time period from 2009 to 2013 (March 16th to May 16th). Using the Kriging interpolation between the temperatures of these seven stations, the T_S is obtained for the whole area (figure 6).

A careful look at the specified area shows that soil temperature at a depth of 5 cm is at higher levels, especially from April 19th to 25th which is the highest level, while the corresponding times in the previous years show the lowest level. This leads to the conclusion that the pattern for 2013 is a seasonal pattern that has also been repeated in the previous years and is caused by a climate cycle.

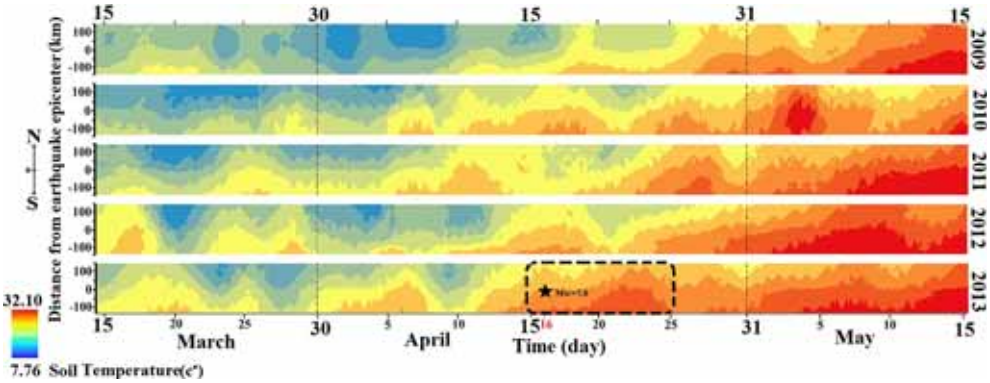

Figure 6. A system of the soil temperature time–space–temperature coordinates, the temperature is automatically related to place and can be interpolated through the location. The region which is marked with black dots shows thermal anomalies.

However, a considerable change from April 19th to 25th can be seen. This change does not follow the pattern and can be related to the earthquake.

Generally, in the time series methods, thermal anomalies can be seen in the time period of the earthquake. These detected anomalies can be expressed as thermal predictors of the earthquake. The results of this research seem to be consistent with those of Akhondzadeh's (2014) and Khalili *et al.* (2019).

Khalili *et al.* (2019) to characterize the thermal anomalies related to the Saravan earthquake, a 10-year specific observation interval of LST data (March 16th to May 16th, every year from 2004 to 2013) were analyzed using Robust Satellite Technique (RST) method. The results showed significant sequences of LST anomalies from several days before and immediately after the Saravan earthquake. Therefore, the results confirmed the existence of space–time thermal anomalies related to destructive earthquakes.

5. Conclusion

In this study, the results of the application of the time series method to five years of satellite data (land surface temperature) and meteorological data (air and soil temperature), were presented. The finding indicates, thermal anomalies in the time period before and after the earthquake, can be seen in all of the mentioned data. In the LST time–space–temperature coordinates, the thermal anomaly pattern can be seen before the Saravan earthquake, especially from April 12th to 16th. In the Kriging surfaces of the air temperature and the ΔT, considerable changes can be seen within the time period from 2 days before the earthquake to 10 days after it. The soil temperature time–space–temperature coordinates, at the depth of 5 cm, show thermal changes (increase) about 3 to 7 days after the Saravan earthquake. The obtained results demonstrate that these changes do not follow the seasonal patterns and are related to the earthquake. Therefore, the results confirmed the existence of space–time thermal anomalies related to destructive earthquakes.

Acknowledgements

The special thanks of the authors to the Manager of the Department of the Meteorology of Sistan and Baluchestan Province, Iran. This study was supported by the Center of Excellence for Environmental Geohazards, and the research council of Shiraz University.

References

Abedi M and Bahroudi A 2016 A geophysical potential field study to image the Makran subduction zone in SE of Iran; *Tectonophys.* **688** 119–134.

Akhondzadeh M 2014 Thermal and TEC anomalies detection using an intelligent hybrid system around the time of the Saravan, Iran, (M_w = 7.7) earthquake of 16 April, 2013; *Adv. Space. Res.* **53(4)** 647–655.

Alavipanah S K, Weng Q, Gholamnia M and Khandan R 2017 An analysis of the discrepancies between MODIS and INSAT-3D LSTs in high temperatures; *Remote Sens.* **9(4)** 347.

Aliano C, Corrado R, Filizzola C, Pergola N and Tramutoli V 2008 Robust Satellite Techniques (RST) for seismically active areas monitoring: The case of 21st May, 2003 Boumerdes/Thenia (Algeria) earthquake; In: *Proceedings of International Workshop on the Analysis of Multi-Temporal Remote Sensing Images IEEE*, pp. 1–6.

Asteriadis G and Livieratos E 1989 Pre-seismic responses of the underground water level and temperature concerning a 4.8 Magnitude Earthquake in Greece on 20 October 1988; *Tectonophys.* **170** 165–169.

Barnhart W D, Hayes G P, Samsonov S V, Fielding E J and Seidman L E 2014 Breaking the oceanic lithosphere of a subducting slab: The 2013 Khash, Iran earthquake; *Geophys. Res. Lett.* **41** 32–36.

Benali A, Carvalho A C, Nunes J P, Carvalhais N and Santos A 2102 Estimating air surface temperature in Portugal using MODIS LST data; *Remote Sens. Environ.* **124** 108–121.

Chandola V, Banerjee A and Kumar V 2009 Anomaly detection: A survey; *ACM Comput. Surv.* (*CSUR*) **41(3)** 15.

Choudhury S, Dasgupta S, Saraf A K and Panda S 2006 Remote sensing observations of pre-earthquake thermal anomalies in Iran; *Int. J. Remote Sens.* **27(20)** 4381–4396.

Cicerone R D, Ebel J E and Britton J 2009 A systematic compilation of earthquake precursors; *Tectonophys.* **476(3–4)** 371–396.

Corrado R, Caputo R, Filizzola C, Pergola N, Pietrapertosa C and Tramutoli V 2005 Seismically active area monitoring by robust TIR satellite techniques: A sensitivity analysis on low magnitude earthquakes in Greece and Turkey; *Nat. Hazards Earth. Syst. Sci.* **5** 101–108.

Crockett R G M and Gillmore G K 2010 Spectral-decomposition techniques for the identification of radon anomalies temporally associated with earthquakes occurring in the UK in 2002 and 2008; *Nat. Hazards Earth Syst. Sci.* **10** 1079–1084.

Di Bello G, Filizzola C, Lacava T, Marchese F, Pergola N, Pietrapertosa C, Piscitelli S, Scaffidi I and Tramutoli V 2004 Robust satellite techniques for volcanic and seismic hazards monitoring; *Ann. Geophys.* **47(1)** 49–64.

Dobrovolsky I R, Zubkov S I and Myachkin V I 1979 Estimation of the size of earthquake preparation zones; *Pure. Appl. Geophys.* **77** 1025–1044.

Eleftheriou A, Filizzola C, Genzano N, Lacava T, Pergola N and Tramutoli V 2016 Long-term RST analysis of anomalous TIR sequences in relation with earthquakes occurred in Greece in the period 2004–2013; *Pure. Appl. Geophys.* **173(1)** 285–303.

Freund F 2003 Rocks that crackle and sparkle and glow: Strange pre-earthquake phenomena; *J. Sci. Exp.* **17(1)** 37–71.

Freund F 2009 Stress-activated positive whole charge carriers in rocks and the generation of pre-earthquake signals, Electromagnetic Phenomena Associated with Earthquakes; Trans world Research Network, Trivandrum, pp. 41–96.

Gholamnia M, Khandan R, Darvishi Boloorani A, Hamzeh S, Gharaylou M, Duan S and Alavipanah S K 2018 Spatiotemporal analysis of diurnal air temperature parameterization in weather stations over Iran; *Desert* **23(1)** 107–121.

Gorny V I, Salman A G, Tronin A and Shilin B B 1988 The Earth outgoing IR radiation as an indicator of seismic activity; *Proc. Acad. Sci. USSR* **301** 67–69.

Guangmeng G and Jie Y 2013 Three attempts of earthquake prediction with satellite cloud images; *Nat. Hazards Earth. Syst. Sci.* **13** 91–95.

Haghipour N, Burg J P, Kober F, Zeilinger G, Ivy Ochs S, Kubik P W and Mohammadi F 2012 Rate of crustal shortening and non-Coulomb behavior of an active accretionary wedge: The folded fluvial terraces in Makran (SE, Iran); *Earth Planet. Sci. Lett.* **355–356** 187–198.

Khalili M and Zamani A 2016 Application of the rule extraction method to evaluate seismicity of Iran; *Geopersia* **6(2)** 233–242.

Khalili M, Alavi Panah S K and Abdollahi Eskandar S S 2019 Using Robust Satellite Technique (RST) to determine thermal anomalies before a strong earthquake: A case study of the Saravan earthquake (April 16th, 2013, M_w = 7.8, Iran); *J. Asian Earth Sci.* **173** 70–78.

Li M and Parrot M 2013 Real time analysis of the ion density measured by the satellite DEMETER in relation with the seismic activity; *Nat. Hazards Earth. Syst. Sci.* **12(9)** 2957–2963.

Lisi M, Filizzola C, Genzano N, Paciello R, Pergola N and Tramutoli V 2015 Reducing atmospheric noise in RST analysis of TIR satellite radiances for earthquakes prone areas satellite monitoring; *Phys. Chem. Earth.* **85–86** 87–97.

Mildrexler D J, Zhao M and Running S W 2011 A global comparison between station air temperatures and MODIS land surface temperatures reveals the cooling role of forests; *J. Geophys. Res. Biogeosci.* **116(G3)**.

Molchanov O A and Hayakawa M 2008 Seismo-electromagnetics and related phenomena: History and latest results (Vol. 190). Tokyo: Terrapub of seismicity in the Iran region; *Geophys. J. Int.* **167** 761–778.

Oliver M A and Webster R 1990 Kriging: A method of interpolation for geographical information systems; *Int. J. Geogr. Inf. Sci.* **4(3)** 313–332.

Ouzounov D, Bryant N, Logan T, Pulinets S and Taylor P 2006 Satellite thermal IR phenomena associated with some of the major earthquakes in 1999–2003; *Phys. Chem. Earth Parts A/B/C* **31(4)** 154–163.

Pavlidou E 2013 Time series analysis of remotely-sensed TIR emission preceding strong earthquakes, Master of Science thesis, Faculty of Geo-information science and earth observation, University of Twente, Enschede, Netherland.

Prigent C, Aires F and Rossow W B 2003 Land surface skin temperatures from a combined analysis of microwave and infrared satellite observations for an all-weather evaluation of the differences between air and skin temperatures; *J. Geophys. Res. Atmos.* **108(D10)**.

Pulinets S A, Ouzounov D, Karelin A V, Boyarchuk K A and Pokhmelnykh L A 2006 The physical nature of thermal anomalies observed before strong earthquakes; *Phys. Chem. Earth* **31** 143–153.

Pulinets S 1997 Radon and metallic aerosols emanation before strong earthquake and their role in atomosphere and ionosphere modification; *Adv. Space. Res.* **20(11)** 2173–2176.

Qiang Z J, Chang-gong D, Lingzhi L, Min X, Fengsha G, Tao L, Yong Zh and Manhong G 1999 Atellitic thermal infrared brightness temperature anomaly image – short-term and impending earthquake precursors; *Sci. China* **42(3)** 313–324.

Qiang Z J, Xu X D and Chang-gong D 1997 Thermal infrared anomaly precursor of impending earthquakes; *Pure. Appl. Geophys.* **149(1)** 159–171.

Quittmeyer R C and Jacob K H 1979 Historical and modern seismicity of Pakistan, Afghanistan, northwestern India and southeastern Iran; *Bull. Seismol. Soc. Am.* **69(3)** 773–823.

Rashki A 2012 Seasonality and mineral, chemical and optical properties of dust storms in the Sistan region of Iran, and their influence on human health. Ph.D. Thesis, Faculty of natural and agricultural sciences, University of Pretoria, South Africa.

Saber Mahani S and Khalili M 2019 Consideration of the soil temperature anomaly before the earthquakes using three filters (Fourier, Wavelet and Difference Logarithmic Filters). *Iranian J. Earth Sci.* **11** 1–16.

Saraf A K, Rawat V, Choudhury S, Dasgupta S and Das J 2009 Advances in understanding of the mechanism for generation of earthquake thermal precursors detected by satellites; *Int. J. Appl. Earth Obs. Geoinf.* **11(6)** 373–379.

Schluter H U, Prexl A, Gaedicke C, Roeser H, Reichert C, Meyer H and Von D C 2002 The Makran accretionary wedge: Sediment thicknesses and ages and the origin of mud volcanoes; *Mar. Geol.* **185** 219–232.

Sulce A 2013 Is land surface temperature an earthquake precursor? Master of Science thesis, Geospatial Technologies, Universidade Nova de Lisboa, Lisbon, Portugal.

Tabari H, Talaee P H, Nadoushani S M, Willems P and Marchetto A 2014 A survey of temperature and precipitation based aridity indices in Iran; *Quat. Int.* **345** 158–166.

Tramutoli V, Corrado R, Filizzola C, Genzano N, Lisi M and Pergola N 2015 From visual comparison to Robust Satellite Techniques: 30 years of thermal infrared satellite data analyses for the study of earthquake preparation phases; *B. Geofis. Teor. Appl.* **56(2)** 167–202.

Tronin A A, Biagi P F, Molchanov O A, Khatkevich Y M and Gordeev E I 2004 Temperature variations related to earthquakes from simultaneous observation at the ground stations and by satellites in Kamchatka area; *Phys. Chem. Earth Parts A/B/C* **29(4)** 501–506.

Tronin A A, Hayakawa M, Molchanov O A 2002 Thermal IR data application for earthquake research in Japan and China; *J. Geodyn.* **33(4–5)** 519–534.

Vernant P H, Nilforoushan F, Hatzfeld D, Abbasi M R, Vigny C, Masson F, Nankali H, Martinod J, Ashtiani A, Bayer R, Tavakoli F and Chery J 2004 Present day crustal deformation and plate kinematics in the Middle East constrained by GPS measurements in Iran and Northern Oman; *Geophys. J. Int.* **157** 381–398.

Wan Z 2008 New refinements and validation of the MODIS land-surface temperature/emissivity products; *Remote Sens. Environ.* **112(1)** 59–74.

Wan Z 2006 MODIS land surface temperature products users' guide. Institute for Computational Earth System Science, University of California, Santa Barbara, CA.

Wan Z and Dozier J 1996 A generalized split-window algorithm for retrieving land-surface temperature from space; *Geosci. Remote Sens. IEEE Trans.* **34** 892–905.

Zamani A, Sami A and Khalili M 2012 Multivariate rule-based seismicity map of Iran: A data-driven modeling; *Bull. Earthq. Eng.* **10** 1667–1683.

Zamani A, Khalili M and Gerami A 2011 Computer-based self-organized zoning revisited: Scientific criterion for determining the optimum number of zones; *Tectonophys.* **510** 207–216.

ZiQi G, ShuQing Q, Chao W, Zhi L, Xing G, Weiguo Z and Jishuang Q *et al.* 2002 The mechanism of earthquake's thermal infrared radiation precursory on remote sensing images; In: *IEEE International Geoscience and Remote Sensing Symposium IGARSS'02* (**4**) 2036–2038.

Corresponding editor: Piyush Shanker Agram